Use of a low-cost phase change material emulsion in de-centralized thermal energy storage for district heating network enlargement

Giulia Rinaldi [a], Ana Lazaro [b], Monica Delgado [b,c,*], Jose Maria Marin [b], Vittorio Verda [a]

[a] *Energy Department, Politecnico di Torino, C.so Duca Degli Abruzzi 24, 10129, Torino, Italy*
[b] *Aragón Institute for Engineering Research (I3A), Thermal Engineering and Energy Systems Group, University of Zaragoza, Agustín de Betancourt Building, C/María de Luna 3, 50018, Zaragoza, Spain*
[c] *Centro Universitario de La Defensa, Academia General Militar, Ctra Huesca S/N, 50090, Zaragoza, Spain*

ARTICLE INFO

ABSTRACT

A detailed heat transfer model of a storage tank was developed to assess the performance of a district heating system with de-centralized storage solutions. The performance of two cases, with water and a low-cost phase change material emulsion as storage medium was analysed for 40 residential buildings in Zaragoza (Spain). The chosen configuration is a typical cylindrical tank with internal coils through which the district heating water flows for the charge and discharge. This decentralized thermal energy storage unit reduced peak demand and mass flow in the network, allowing additional buildings to connect to a saturated grid. Four configurations were examined: (1) A 180 m^3 water tank reduced district heating power demand by 36.6 %. (2) The same 180 m^3 tank using the emulsion required fewer coils, lowering costs, stabilizing TES temperature, and increasing water supply temperature, thus extending system lifespan. (3) A 130 m^3 tank with the emulsion offered operational characteristics similar to the water tank, with economic and structural benefits from reduced size. (4) An 180 m^3 optimised tank with the emulsion achieved a 38.8 % reduction in district heating power demand. These configurations demonstrate the efficiency and cost-effectiveness of using phase change material emulsion in thermal energy storage systems.

1. Introduction/background

District heating (DH) presents a widely accepted method for supplying heat to buildings situated within densely populated urban regions. This approach revolves around generating heat for residential heating via centralized facilities, diverging from individual household boilers. Such centralized production enhances overall efficiency [1]. Typically, DH systems consist of one or more thermal plants and an interconnected network of insulated pipes through which hot water, superheated water, or steam is conveyed, delivering heat to end users. The types of thermal plants utilized in DH systems have undergone significant evolution over the past four decades. In the early 21st century, the primary focus concerning DH system advancement centres on transitioning to more sustainable systems characterized by reduced or zero carbon emissions [2].

The current trend when designing DH systems is based on low [3,4] and ultra-low temperature heat carriers [5], also named as 4th and 5th

generation DH systems respectively. Low Temperature District Heating (LTDH) can operate in the range between 50 and 55 °C to 60-70 °C supply and 25-30 °C to 40 °C return temperatures and meet consumer demands for space heating and domestic hot water (DHW) demands. These LTDH complies with two main requirements for future DH: increase the efficiency of technologies for heat production and high share of renewable energy, often available at low temperature [6]. Given the intermittent nature of renewable heat sources, they may not always align with heat demand. Therefore, integrating thermal energy storage (TES) technologies into LTDH networks is crucial to bridge the gap between the heat supply and demand. TES can be classified depending on the storage duration as short-term and long-term storage for hourly/daily and seasonal storage respectively. In turn, these TES systems can be classified according to the physical phenomenon involved as sensible, latent or chemical storage [7]. If focus is on short-term TES, these can be integrated either at DH buildings' substations, generally called distributed TES, or at strategic locations along the grid outside any producers (de-centralized) or close to the heat generation facility

* Corresponding author. Aragón Institute for Engineering Research (I3A), Thermal Engineering and Energy Systems Group, University of Zaragoza, Agustín de Betancourt Building, C/María de Luna 3, 50018, Zaragoza, Spain.
E-mail address: monica@unizar.es (M. Delgado).

Nomenclature

A	Area [m^2]
C $\equiv \dot{m}c_p$	Heat capacity [W/K]
c_p	Specific heat capacity [J/kg/K]
D or d	Diameter [m]
E	Thermal energy [J]
EA	Thermal energy stored [J]
f	frequency [Hz]
g	Acceleration of gravity [m/s^2]
h	Specific enthalpy [J/kg]
H	Height [m]
L	Length [m]
m	Mass [kg]
$\dot{m}$	Mass flow [kg/s]
N	Number of days, coils, revolutions per minute [−]
Q	Heat [J]
$\dot{Q}$	Heat rate [W]
R or r	Radius [m]
s	Thickness [m]
T	Temperature [°C]
t	time [s]
U	Overall heat transfer coefficient [W/m^2/K]
u	Specific internal energy [J/kg]
V	Volume [m^3]
v	Velocity [m/s]

Greek symbols

α	Convection heat transfer coefficient [W/m^2/K]
β	Thermal expansion coefficient [K^{-1}]
$\dot{\gamma}$	Shear rate [s^{-1}]
δ or Δ	Variation of (used with other physical dimensions) [−]
ε	Heat exchanger effectiveness [−]
η	Efficiency [−]
λ	Thermal conductivity [W/m/K]
μ	Viscosity [Pa·s]
ν	Kinematic Viscosity [m^2/s]
ρ	Density [kg/m^3]

Dimensionless numbers

Nu	Nusselt number [−]
Pr	Prandtl number [−]
Ra	Rayleigh number [−]
Re	Reynolds number [−]

Subscripts

av	Average
d	Demand
e	External
em	Emulsion
env	Environment
HE	Heat exchanger
h	Hourly
i	Internal
in	Inlet
ins	Insulation
loss	Heat loss
max	Maximum
min	Minimum
net	DH network
nom	Nominal
op	Operation
out	Outlet
r	Return
st	Stirrer
sto	Storage
s	Supply
w	Water

Abbreviations and brackets

CHP	Combined Heat and Power
DH	District Heating
DHW	Domestic Hot Water
EA	Energy Accumulated
LTDH	Low Temperature District Heating
NTU	Number of Transfer Units
PCM	Phase Change Materials
PHE	Plate Heat Exchanger
RHD $\equiv H/D$	Tank shape ratio
SH	Space Heating
TES	Thermal Energy Storage
[m]	Monthly average
[h]	Hourly

(centralized) [8]. In the literature, numerous studies focus on sensible TES in DH networks, while relatively few address latent TES.

In 2012, a study was conducted where a TES unit for DH networks was designed and characterized using Computational Fluid Dynamics (CFD). The system employed a shell-and-tube configuration containing a commercial paraffin, RT100. This study also included an analysis of the possible system configurations compared to sensible energy storage systems, focusing on temperature differences and energy storage density terms [9]. Subsequently, in 2017, Castro et al. conducted a comparative techno-economic analysis of short-term latent TES for DH applications. The TES system was positioned parallel to the substation primary side, requiring a phase change temperature of 70 °C. Due to limited thermal discharge power output, a supplementary heater was necessary. The analysis revealed that the latent TES costed four times more than sensible TES systems utilizing water [10]. In 2022, the integration of a latent TES into a small-scale DH network consisting of 126 apartments was studied. The TES employed a shell-and-tube heat exchanger using a Phase Change Material (PCM) with a melting temperature close to 80 °C, which proved crucial for peak load shifting of hot water in the apartment complex [11]. More recently, in 2023, a latent TES was developed and dimensioned for a DH network, utilizing a paraffin with a phase change temperature of 70 °C contained in spherical capsules, through numerical modelling. This model enables district network designers to dimension, optimize, and predict the dynamic behaviour of the TES under real operating conditions. Additionally, the integration of the TES system into a real DH network in Grenoble, France, was analysed, although specifics of the integration were not provided [12].

When new areas with low-energy buildings are built, additional districts may be connected to the existing LTDH network and the integration in LTDH expects the enhancement of the building energy efficiency (better insulations, low-T SH systems, lower heat losses, etc.) and the substitution of the boiler units with the DH substations.

An increased number of buildings supplied by the DH systems implies a higher heat demand that the network has to satisfy. Dealing with traditional Combined Heat and Power (CHP)-based DH system, this can be achieved by means of a raised temperature or mass flow of the supply water according to the overall system control strategy. Usually, the overall DH system is regulated through the combination of four control systems [13]: 1) heat demand control, 2) flow control, 3) differential pressure control and 4) supply temperature control.

While the heat demand control is placed into the buildings, the space heating (SH) flow control is accomplished by a valve situated on the secondary circuit after the heat exchanger. The supply temperature control, as well as the supply flow control, is managed by the heat supply unit in order to provide the necessary thermal power to the consumers.

In this work, the integration of de-centralized TES with PCM emulsion into LTDH system is analysed with a double purpose: i) the "peak shaving" of the heat demand and ii) the connection of new buildings/ districts to the already existing LTDH networks, a troublesome procedure that adjust the supply water temperature provided to the DH. The set point value has to respect the minimum limit and it is dependent on the outdoor temperature. However, the high thermal inertia of the DH network makes difficult to change continuously the supply temperature for satisfying the heat demand. On the flow control side, at any given load, the corresponding water flow is discharged according to the actual supply temperature level [14].

Dealing with LTDH, the networks are designed based on the maximum estimated hydraulic load, considering a supply temperature about 55 °C and a maximum allowed water velocity into the pipe around 2 m/s. This temperature level might be sufficient all-year round with the exception of some high peak periods [15]. If the existent DH grid is already hydraulically saturated, no additional areas can be integrated. Consequently, the enlargement of the system would imply the replacement of most part of the distribution pipes. Therefore, this study proposes the integration of a de-centralized storage tank containing a low cost PCM emulsion, as a feasible solution. This approach aims to avoid the reconstruction of the distribution network and enable the connection of new dwellings. The study employed a mathematical model to analyse the behaviour of the system, comparing it to the integration to a de-centralized water tank, setting as objective the minimization of the tank volume and the minimization of the DH nominal power demanded. While latent TES have garnered significant interest in the literature, there are notably few examples addressing its application within DH systems, as already mentioned. To the best of our knowledge, none of these examples explored decentralized latent TES solutions or their integration for DH network enlargement. Furthermore, the utilization of a PCM emulsion for the purposes described remains unexplored, despite its potentially superior thermal response compared to conventional latent TES systems [16]."

2. Decentralized TES simple model

2.1. Thermal energy storage materials: PCM emulsion

While the technical feasibility of TES solutions with PCMs has been widely demonstrated, their economic feasibility remains a concern. Hence, a low cost PCM emulsion has been proposed. The PCM emulsions are mixtures of small droplets of PCM dispersed in water as continuous phase [17]. Despite the solid-liquid change of the dispersed phase, the product is always in the liquid state, which facilitates its integration and use into simple and cost-effective storage tanks. The emulsified PCM is a low-cost paraffin, specifically a by-product of the petroleum refining process. According to the technical specifications supplied by the manufacturer, the solids content of this PCM emulsion is about 60 % with an average particle size of 1 μm. Their thermophysical and rheological properties had already been experimentally tested previously to this study [16]. The phase change occurs in the temperature range of 30-50 °C, which aligns precisely with the requirements of the decentralized TES unit for a LTDH network. The enthalpy change between phases is 140 kJ/kg. Although the PCM emulsion exhibits significant hysteresis, which could compromise the operation of the proposed system, this aspect has not been considered in the model presented in the subsequent sections. In fact, the supplier of the PCM emulsion is working to reduce this hysteresis phenomenon, which is common in this type of fluid. The measured density range of the PCM emulsion is 0.9372 kg/m^3 at 20 °C- 0.8704 kg/m^3 at 60 °C. In relation to the thermal conductivity,

Table 1
Compilation of the measured PCM emulsion properties, together with the methodology adopted and the measurement uncertainty.

Property	Equipment/methodology	Uncertainty
Enthalpy	T-history installation: built by the authors	5 %
	Differential Scanning Calorimeter: Netzsch, DSC 200 F3 Maia	1 %
Viscosity	Controlled stress rheometer: TA Instruments, AR-G2	5 %
Density	Oscillating U-tube densimeter: Mettler Toledo, DM40	<1 %

thermal diffusivity was measured with a Laser Flash Apparatus, however results were not reliable enough. LFA is a technique to measure thermal diffusivity on solid samples, and although LFA manufacturers have developed special liquid sample holders [18], there is still a great uncertainty associated with the measurement [19]. For that reason, a constant value of 0.4 W/(m K) has been considered for the thermal conductivity of the PCM emulsion, according to the Maxwell's relationship, knowing that it is not a dilute dispersion [20]. The viscosity is also relevant to know the convective phenomenon inside the storage, as well as inside heat exchangers or tubes. The PCM emulsion shows a pseudoplastic behaviour and its viscosity ranges between 0.11 and 0.14 Pa s at 100s^{-1} for a temperature range between 20 and 40 °C. The equipment and uncertainties associated with the measurements are compiled in Table 1.

2.2. Heat demand

The optimal operation of a DH system depends on the accuracy of the thermal load estimation; predictive models allow forecasting reliable demand data based on the relationship between the thermal load and the outdoor temperature [21]. Given the substantial fluctuations in energy demands within residential buildings, hourly demand data becomes imperative for precise energy system assessments. However, conducting hourly simulations spanning an entire year could incur impractical computational costs. To address this challenge, a widely adopted approach involves reducing the simulation period to a subset of days, focusing solely on representative typical days, properly selected to represent the whole year [22]. The SH demand data handled in this study are measured data registered in the Zaragoza "Goya" district, where one representative day is considered for each month (Fig. 1). It has been assumed a hypothetical additional connection to the existing grid of 500 dwellings presenting the same thermal profile of the monitored flats, distributed in twenty buildings with twenty-five apartments each one For this expansion, the current DH network has to be adequate for bearing the increased hydraulic load. The shape of the curves appears similar in all the months: the highest daily peak is verified at the 7th hour and other increment occurs starting from the 17 h, whose shape changes according to the month. Since the 23rd hour until the 6th hour, the in-house space heating systems are usually switched off and the circulating DH mass returns without discharging heat. Due to the necessity and the interest to work with LTDH, the reduced working temperature can be not adequate for traditional DHW preparation methods. For that reason, it has been considered an amplification of the DH grid just for SH supply.

To avoid the oversizing of the components of the new connection due to the peak demands, it is necessary to take from the DH only the average demand. The target is to store the surplus heat during the day intervals with a demand, Q_h, minor than the average, Q_{av}, and to recover it in the intervals with a demand greater than the average. Thanks to the storage, the DH supply temperature (55 °C) can be kept constant, while a nominal mass flow would be established in each month.

2.3. Methodology

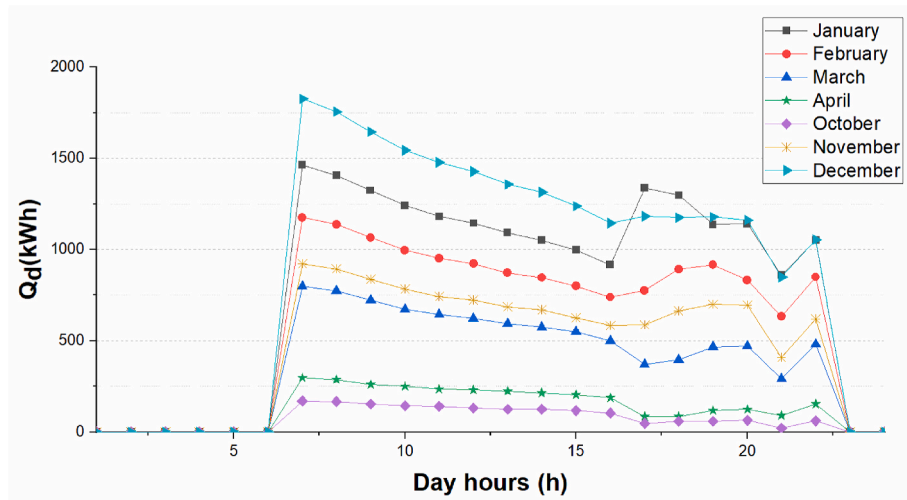For the sake of simplicity, it is first considered as reference the case

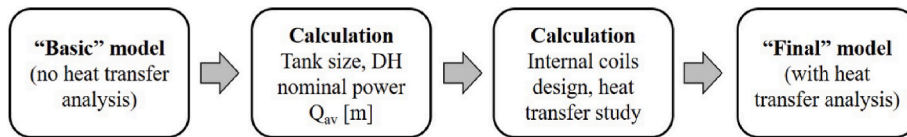**Fig. 1.** SH demand for 20 buildings in a Zaragoza district.

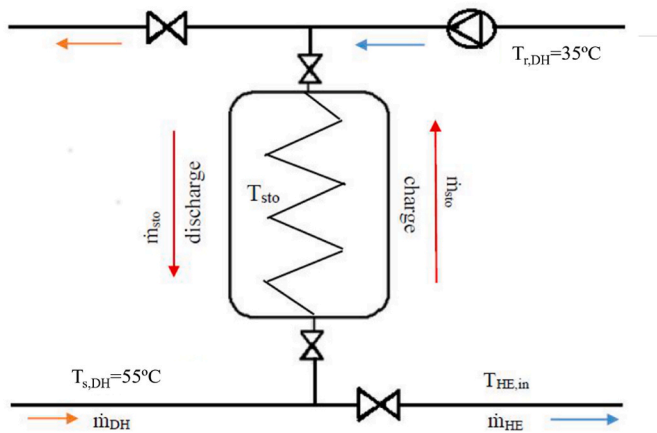**Fig. 2.** Procedure for the elaboration of the de-centralized TES model.

Fig. 3. De-centralized TES connection scheme with DH grid.

Fig. 4. DH mass profile throughout the year.

with water as storage medium, and afterwards the case of a PCM emulsion. The equations of the model are the energy and mass balances that defined the regulation necessary for achieving the desired operation of the storage and the heat transfer kinetics.

Due to the interest in LTDH, as previously explained, the reduced working temperature can be not adequate for traditional DHW preparation methods. For this reason, it has been considered an amplification of the DH grid to provide the new SH supply, making for example the assumption that other innovative techniques (solar thermal, heat pumps, etc.) could be exploited for the DHW.

2.3.1. Ideal tank model

To determine the TES unit adequate to fit the storage necessities, the algorithm shown in Fig. 2 has been followed. The way of avoiding taking into account the heat kinetics is to suppose a perfect efficiency of the charge and discharge processes, that is, by supposing that the water leaves the storage tank at the storage temperature, T_{sto} (Fig. 3). Since one
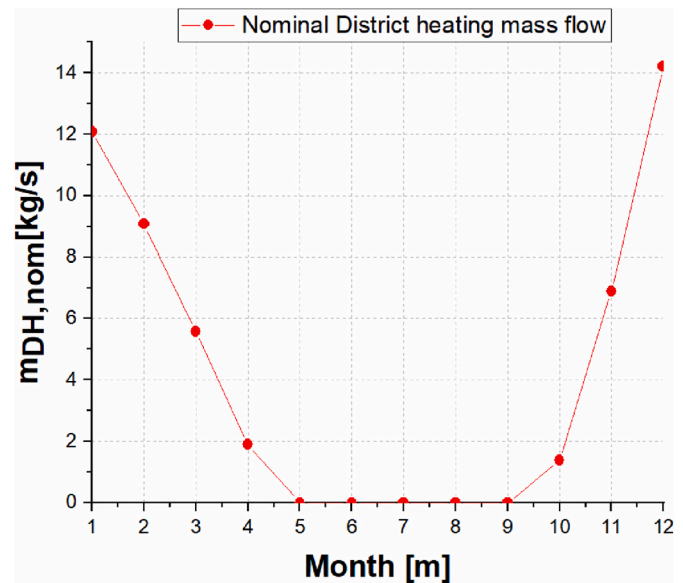
of the objectives of the TES is to facilitate the DH regulation, the DH supply temperature, $T_{s,DH}$, has been conserved constant along the whole working period and equal to 55 °C.

Without a TES unit, the heat power unit controls the DH energy delivered to any branch by varying the mass flow, within the allowed limits; the inclusion of the TES allows keeping constant the mass flow, $\dot{m}_{DH}$, during each whole month. In order to limit the temperature fluctuations on the return DH side and guarantee the adequate energy discharged into the heat exchanger at customers substation, the return temperature of the water just after the plate heat exchanger (PHE), $T_{r,DH}$, has been set to be 35 °C. For the lower temperature heating terminal units, usual values can be assigned to the supply and return tempera-
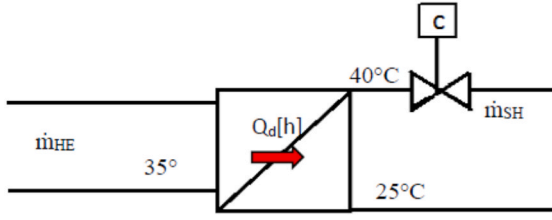
Fig. 5. Building substation scheme with related variables.

tures, $T_{s,SH} = 40\ °C$ and $T_{r,SH} = 25\ °C$. Once fixed the temperature variations of the heat carrier, the nominal mass flows in both primary and secondary circuits are determined for each monthly average heat demand according to equations (1) and (2):

$$\dot{m}_{DH,nom}[m] = \dot{Q}_{av}[m] \,/\, [c_{pw}(T_{s,DH} - T_{r,DH}] \qquad (\text{Eq. 1})$$

$$\dot{m}_{SH,nom}[m] = \dot{Q}_{av}[m] \,/\, [c_{pw}(T_{s,SH} - T_{r,SH})] \qquad (\text{Eq. 2})$$

The average heat space demand in the studied dwellings need the nominal values given in Fig. 4.

From equations (1) and (2) and the values assigned to the supply and return temperatures of both circuits, it is deduced that both mass flows are related by $\dot{m}_{DH,nom} = 0.75\,\dot{m}_{SH,nom}$. The actual mass flow, $\dot{m}_{SH}$, needed to meet the hourly demand is given by equation (3):

$$\dot{m}_{SH}[h] = \dot{Q}_d[h] \,/\, [c_{pw}(T_{s,SH} - T_{r,SH})] \qquad (\text{Eq. 3})$$

and changes hourly. As this value cannot be lower than a minimum, $\dot{m}_{min}$, for a proper operation of the pumps and the heat exchanger, if the result of equation (3) is less than $\dot{m}_{min}$, the operating time interval, Δt, of the secondary circuit should be calculated as $\Delta t = (\dot{m}_{SH}[h]\,/\,\dot{m}_{min})\cdot 1$ h. Δt is less than 1 h only for some time intervals of the months with very low demands, like April and October; for the rest of the time, $\Delta t = 1$ h.

The operation mode of the storage in each hour [h] is defined by the comparison between the nominal fixed $\dot{m}_{SH,nom}[m]$ and the current value of $\dot{m}_{SH}[h]$. Fig. 5 shows the configuration of a building's substation with the main variables involved.

By comparing the nominal and the actual mass flows, one of the two following situations is given.

a) Charge of the TES

If $\dot{m}_{SH}[h] < \dot{m}_{SH,nom}[m]$, the DH provides excessive thermal power and only the portion of its mass flow given by $\dot{m}_{HE}[h] = Q_d[h]/[\Delta t\cdot c_{pw}\cdot(T_{s,DH} - T_{r,DH})]$ must be sent to the heat exchanger and the remaining part (equation (4)),

$$\dot{m}_{DH,nom}[m] - \dot{m}_{HE}[h] = \dot{m}_{sto}[h] \qquad (\text{Eq. 4})$$

is driven to the storage tank, taking place a charge process. The energy stored during the hour is given by equation (5):

$$E_{sto}[h] = \dot{m}_{sto}c_{pw}(T_{s,DH} - T_{sto}[h])\Delta t + \dot{m}_{DH,nom}c_{pw}(T_{s,DH} - T_{sto}[h])(1 - \Delta t) \qquad (\text{Eq. 5})$$

and the total energy accumulated (EA) at any hour, $EA[h]$ is according to equation (6):

$$EA[h] = E_{sto}[h] + EA[h - 1] - Q_{loss}[h] \qquad (\text{Eq. 6})$$

where $Q_{loss}[h]$ are the losses through the walls of the tank, the variation of the internal energy of the storage substance at any hour is $\Delta u[h] = (E_{sto}[h] - Q_{loss}[h])/(\rho_{sto}V_{sto})$ and, by means of dependence of u with the temperature, the mean storage temperature, T_{sto}, can be determined.

b) Discharge of the TES

If $\dot{m}_{SH}[h] > \dot{m}_{SH,nom}[m]$, the DH can only provide one fraction of the thermal demand and the remaining $Q_d[h] - Q_{av}[m] = Q_{sto}[h]$ is taken from the TES. The mass flow of DH return that must be passed through the storage tank and added to the flow coming from DH supply is given by equation 7

$$\dot{m}_{sto}[h] = Q_{sto}[h] \,/\, [\Delta t\cdot c_{pw}\cdot(T_{sto}[h] - T_{r,DH})] \qquad (\text{Eq. 7})$$

This mass flow is withdrawn from the return pipe thanks to the work of a pump activated by a flow switch. equation (6) and the same procedure for the charge case is used to compute the thermal energy stored and the temperature of the storage medium at each hour of the day. In this case, it has to be checked that the storage has not been totally discharged (equation (8)).

$$EA[h] = max(EA_x[h], 0) \qquad (\text{Eq. 8})$$

The mass flow that the PHE has to handle into the primary side is the sum of the nominal DH and that given by equation (9). Since the temperature of the storage is kept always lower than $T_{s,DH}$, $\dot{m}_{sto}[h]$ presents a lower temperature than the district water, generating a decrease of the inlet PHE temperature (Equation (10)).

$$\dot{m}_{HE}[h] = \dot{m}_{sto}[h] + \dot{m}_{DH}[m] \qquad (9)$$

$$T_{HE,in}[h] = (\dot{m}_{sto}[h]\,/\,\dot{m}_{HE}[h])T_{sto}[h] + (\dot{m}_{DH}[m]\,/\,\dot{m}_{HE}[h])T_{s,DH} \qquad (\text{Eq. 10})$$

An adequate value of $T_{HE,in}[h]$ has to be always ensured. Its excessive reduction could imply the undesirable effectiveness drop of the PHE into the customers' substation. Although, even with a minimum $T_{HE,in}[h]$ constraint of 45-44 °C, it is already accepted a performance reduction during the discharging time.

2.3.2. Real tank model

To determine the actual behaviour of a system TES-DH, a more detailed model of the storage tank must be established. The chosen configuration is a typical cylindrical tank with internal coils through which the DH water flows to carry out the charge and discharge processes. The nominal power has been determined attempting to achieve the highest reduction in relation to the peak; using higher tank sizes allows attaining lower primary flow, but the combination of tank volume and nominal DH power in each month has to guarantee two conditions.

a) $T_{HE,in}[h] \geq T_{HE,in,min} = 44 - 45\ °C$.
b) No auxiliary heat demand or heat rejection.

With a more detailed model that evaluates the actual heat transfer efficiency between the storage medium and the coils, lower $T_{HE,in}[h]$ will be obtained. Therefore, to keep the same monthly nominal DH

Table 2

$\dot{Q}_{av}$ [m] estimated with $V_{sto} = 160\ m^3$ and corresponding reduction relative to $\dot{Q}_{peak}$ [m].

	January	February	March	April	October	November	December
$\dot{Q}_{av}$/ kW	1010.0	760.0	465.0	160.0	120.0	580.0	1190.0
$\dot{Q}_{peak}$/ kW	1462.9	1176.1	798.4	298.0	171.1	920.6	1823.0
% Red	30.96	35.38	41.76	46.31	29.87	37.00	34.72

loads, the tank dimension will have to be slightly risen in order to restore the desired value of $T_{HE,in,min}$. Due to this issue, the volume has been selected with a reasonable margin for not overpassing V_{max} (200 m³ due to reasons of investment costs) in a future variation. The effective volume value considered as suitable for the studied case has been 160 m³ (with water as storage medium, "basic" model). The term *effective* means *occupied with the storage substance*, so that to this number the volume occupied by the coils must be added to get the actual volume of the tank. The basic model has been implemented for each month several times in order to meet the value of $\dot{Q}_{av}[m]$ that respects the imposed restrictions. In Table 2 the nominal DH power values recommended for meeting the SH demand of the studied additional buildings are listed, exploiting a TES with an effective volume of 160 m³. A very noticeable reduction of the thermal demand to the DH system, and therefore of the mass flow, is accomplished.

December and January are the months with the highest demand and where the storage is more exploited; however, in order to provide the required $T_{HE,in}$, the storage cannot be discharged completely and, therefore, the DH has to deliver more energy. Consequently, in these months, it has not been possible to establish a nominal value diminished of the same entity accomplished for the others. Another problematic month arose to be October because of its very low demand. Indeed, for guaranteeing the minimum secondary flow, the floor-heating works for less time, influencing the whole performance and operation of the system.

To size the coils, the largest mass flow of water passing into the tank must be known. The solution of the former system of equations gives as one of its results that the largest mass flow happens in January at the end of the discharge when the storage temperature is lower. By choosing a proper standard diameter and a proper velocity of the water, equation (11) allows calculating the number of coils needed.

$$N_{coils} = 4\, \dot{m}_{max,sto} \left/ \left(\pi D_i^2 \rho_w \nu_w \right) \right. \cong 20 \qquad \text{(Eq. 11)}$$

The length of the coils is determined by the heat transfer required between the coils and the medium stored in the tank. As the heat capacity of water flowing inside the coils is much lower than the average heat capacity of the storage medium during the phase change of the PCM emulsion, the expression that gives the efficiency of the heat exchange is (equation (12)):

$$\varepsilon = 1 - exp(-NTU) \qquad \text{(Eq. 12)}$$

To reach a ε high value, the target value of the number of transfer units must be higher than 1.5. But this number depends on the internal, α_i and external, α_e, convection coefficients through the global transmission coefficient, U, given by equation (13), where D_e and D_i are the external and internal diameter of the coil tube:

$$U_e^{-1} = (D_e / D_i)\alpha_i^{-1} + \alpha_e^{-1} + D_e\, ln\big((D_e / D_i) / (2\lambda_{coil})\big) \qquad \text{(Eq. 13)}$$

The value of α_i can be computed by any proper experimental correlation, such as the given by Rogers and Mayhew (equation (14)) [23]:

$$Nu_i = 0.021\, Re_i^{0.85} Pr_{wall}^{0.4} (D_i / D_{coil})^{0.1} \qquad \text{(Eq. 14)}$$

By assuming that the temperature of the water contained into the tank is uniform and changes with time depending on the charge and discharge processes, the external convection is natural and its coefficient can be computed with equation (15) [24]:

$$Nu_e = 0.5\, Ra^{0.2633} \qquad \text{(Eq. 15)}$$

where the Rayleigh number is defined as usually, $Ra \equiv g\beta(T_{coil} - T_{sto})D_e^3 / \nu^2 \cdot Pr$.

The heat transfer parameters obtained are: $\alpha_{i,max} = 5415$ W/m²K, $\alpha_{e,av} = 912.4$ W/m²K, $U = 757.4$ W/m²K, $\dot{m}_{max,coil} = 0.92$ kg/s.

On the side of the water contained into the tank, its temperature can be obtained by equation (16):

Table 3
Heat transfer and coil design results.

Heat transfer parameters		Coil dimensions	
$\alpha_{i,max}$	5415.0 W/(m²·K)	d_e	0.03801 m
$\alpha_{e,av}$	912.4 W/(m²·K)	L_{coil}	80 m
U	757.4 W/(m²·K)	D_{coil}	0.6 m
$\dot{m}_{max,coil}$	0.92 kg/s	N_{coils}	20

$$(\rho V c_p)_{sto} \frac{dT_{sto}}{dt} = \dot{Q}_{sto} = (\dot{m}c_p)_w (T_{w,i} - T_{w,o}) = (\dot{m}c_p)_w \varepsilon (T_{w,i} - T_{sto}) \qquad \text{(Eq. 16)}$$

where

$$\frac{(\rho V c_p)_{sto}}{(\dot{m}c_p)_w} \frac{dT_{sto}}{dt} = \varepsilon (T_{w,i} - T_{sto}) \qquad \text{(Eq. 17)}$$

To end with the design, the length of the coils must be calculated according to the desired number of transfer units (NTU) (equation (19)).

$$L_{coils} = NTU \cdot \dot{m}_{max,sto} c_{pw} \left/ (U_e N_{coils} \pi D_e) \right. \qquad \text{(Eq. 19)}$$

By applying the previous formulae, the results shown in Table 3 are obtained.

2.3.3. Sizing and operating the TES

At the beginning of each hourly interval, $\dot{m}_{SH,nom}[m]$ and $\dot{m}_{SH}[h]$ are evaluated by means of equations (1) and (2) and compared. The sign of their difference decides if a charge or discharge process must be carried out. In either case, equation (4) or 7 determines the mass flow to be passed through the storage tank, and the ratio $N_{coils,op}[h] = \dot{m}_{max,sto}[m]/\dot{m}_{sto}[h]$ indicates the number of coils that must be put into operation to keep the heat transfer efficiency and a proper performance of the whole system.

Each month, the average difference between storage temperature and the approximated value of the coiled tube wall has been calculated in order to estimate the average effectiveness to be used. Although the actual temperature difference changes each hour, the use of an average value for the calculation of the Rayleigh number allows decreasing the computation effort achieving a satisfactory simulation of the whole system performance. The heat transfer efficiency reached with the selected internal coils is about 0.85–0.86, depending on the month. The effectiveness determines the outlet temperature that can be attained by the water flow circulating into the TES (equation (20)). Taking into account the heat transfer, the actual temperature variation of the water temperature in the coils ($T_{w,o}[h] - T_{w,i}[h]$) has substituted the ideal one, $T_{sto}[h]$, employed in the "basic model".

Charge: The temperature of the water leaving the tank is given by

$$T_{w,o}[h] = T_{s,DH} - \varepsilon (T_{s,DH} - T_{sto}[h]) \qquad \text{(Eq. 20)}$$

and the stored thermal energy is calculated by means of equation (21):

$$E_{sto}[h] = \dot{m}_{sto}[h]c_{pw}(T_{s,DH} - T_{w,o}[h])\Delta t + \dot{m}_{DH,nom}c_{pw}(T_{s,DH} - T_{w,o}[h])(1 - \Delta t) \qquad \text{(Eq.21)}$$

Discharge: The temperature of the water leaving the tank is given by equation 22:

$$T_{w,o}[h] = T_{r,DH} + \varepsilon (T_{sto}[h] - T_{r,DH}) \qquad \text{(22)}$$

and the mass flow of the return water driven into the tank is calculated by means of equation 23

$$\dot{m}_{sto}[h] = Q_{sto}[h] \left/ \left[\Delta t \cdot c_{pw} \cdot (T_{w,o}[h] - T_{r,DH}) \right] \right. \qquad \text{(Eq. 23)}$$

Finally, the size and insulation of the tank must be fixed. To minimize the storage external area and, therefore, the heat losses, a height-diameter ratio of 1 has been chosen. For the insulation a 5 cm layer of

Table 4
De-centralized TES dimensions and insulation characteristics.

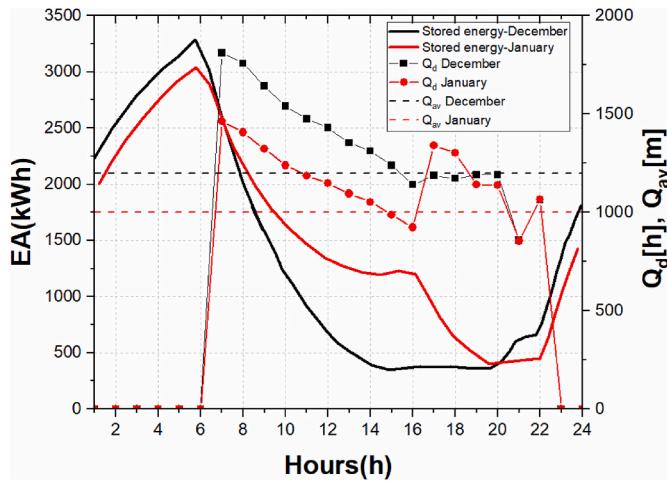| Storage dimensions		Insulation layer	
RHD	1	s_{ins}(m)	0.05
D_{sto}(m)	6.12	λ_{ins}(W/(m·K))	0.024
H_{sto}(m)	6.12	U_{sto} (W/(m²·K))	0.480
A_{sto}(m²)	176.50	T_{env}(°C)	15
$V_{sto,eff}$(m³)	180.00		
V_{sto}(m³)	180.00 + 22·V_{coil}		

Fig. 6. Storage energy and space heating demand daily profile for the representative day of December and January.

polyurethane has been selected. In Table 4 all the variables related to the tank geometry and insulation are listed.

The introduction of the heat transfer effectiveness into the model has slightly affected the charging/discharging phase of the TES. As a consequence, higher storage mass flows are necessary for attaining the same discharging power and the implementation of the final model has resulted in a higher number of coils, 22 instead of 20, conserving the same coil size. In order to maintain the required minimum $T_{HE,in}$ [h], its effective volume has been incremented to 180 m^3. This final model has been implemented for each month in its representative day and the obtained results describe the trend of the variable and the system operation on hourly basis (24 h).

December and January were the months in which the storage would have been exploited more. Indeed, because of their high heat demand, and its more consistent variation throughout the day, the storage unit had been highly charged and discharged. A particular interest offers the comparison between the hourly loading/unloading processes with the space heating demand shown in Fig. 6.

3. De-centralized TES using the PCM emulsion as thermal storage material: the model

The actual storage medium (water) is replaced with a low-cost PCM emulsion. Two major changes come to be: a new h-T curve and the

Table 5
Heat transfer study of the PCM emulsion in a tank with $V_{sto,eff}$ (180 m³) of 14 internal coils.

Geometric variables		Heat transfer	
D_{st}(m)	0.75	Re_e	9196
D_{tank}(m)	1.64	Pr_{em}	3461
D_{coil}(m)	0.80	Nu_e	3774
N_{st}(rpm)	220	α_e(W/(m²·K))	922.7
ε	0.85	U(W/(m²·K))	760.9

changes in heat transfer kinetics, expecting to be worse because of the strong increase in the viscosity. This study starts from the experimental tests performed with the same paraffin emulsion as thermal storage material in a small tank unit with one internal coiled tube [16]. As predicted, the observed drop of the global heat transfer coefficient U was from 500 W/(m²·K) to 100 W/(m²·K), resulting inefficient because of the reduction of the coil effectiveness and of the charging/discharging performance of the TES. To improve this situation, a stirrer is introduced [25].

3.1. Changes in the model

With regard to the thermal storage capacity of the emulsion, it is only necessary to substitute in the previous equations the c_{pw} by the higher value of the thermal capacity given by the measured $h - T$ curves of the emulsion [16]. Concerning the heat transfer between the emulsion and the water as heat carrier, the internal convective heat transfer coefficient, $\alpha_{i,max}$, remains the same, but a mixed convection mechanism dominates the external side of the coil. The correlation proposed by Pollard and Kantyka and defined by equations (24) and (25) is used [26]:

$$Nu_e = 0.077 Re_e^{2/3} Pr^{1/3} \left(\mu_{eff} / \mu_{eff,wall} \right)^{0.14} (D_{tank}/D_e)^{0.48} (D_{coil}/D_e)^{0.27}$$

(Eq. 24)

$$\alpha_e = Nu_e \cdot \lambda_{em} D_{tank}$$

(Eq. 25)

The Reynolds number is defined as $Re_e \equiv \rho f_{st} D_{st}^2 / \mu_{eff}$, where f_{st} is the frequency of rotation in Hz. As the emulsion is a non-Newtonian fluid, its effective viscosity, μ_{eff}, is determined according to the model of Ostwald de Waele (equation (26))

$$\mu_{eff} = K\dot{\gamma}_{eff}^{n-1}$$

(Eq. 26)

where $\dot{\gamma}_{eff}$ is the effective shear rate that, for pseudoplastic fluids, can be computed with equation (27) proposed by Metzner and Otto [27]

$$\dot{\gamma}_{eff} = k_{st} f_{st}$$

(Eq. 27)

being k_{st} an empirical parameter depending upon the shape of the stirrer and of the vessel configuration, given by equation 28

$$k_{st} = \left(9.5 + 9 / \left(1 - (D_{st}/D_{tank})^2 \right) ((3n+1)/4n)^{n/(n-1)} \right)$$

(Eq. 28)

The empirical values for the tested configuration of tank and stirrer are $K = 3.658$ and $n = 0.302$. For a better performance, there are several coils inside the tank and, in order to preserve a good heat transfer rate, each coil has its own stirrer.

It should also be pointed out that given that the convective resistance of the PCM emulsion is dominant and considering equation (25), the overall heat transfer coefficient increases approximately linearly with the thermal conductivity of the PCM emulsion, so it is a fundamental thermophysical property but is limited by the thermal conductivity of the water and the PCM.

3.2. Results of the TES simulation with the PCM emulsion

The utilization of a storage medium with a higher energy density than water contributes to alleviate space difficulties and to stabilize the tank temperature due to the phase transition. As the improvements can be of different kind, several targets can be chosen; three of them have been simulated and applied to three months of relevant behaviour: December by having the most complete charge-discharge cycle; January because of its most greater hourly variations of mass flow, $\dot{m}_{HE,in}$ [h] and $\dot{m}_{sto}$ [h], and inlet temperature to the heat exchanger, $T_{HE,in}$[h]; and finally March as a month with low demand and small fluctuations.
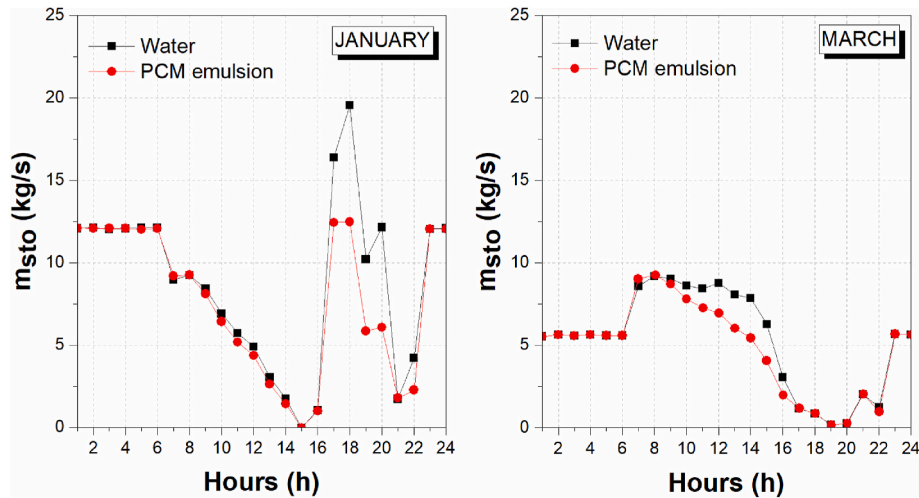
Fig. 7. Mass flow circulating through the storage for January (left) and March (right).
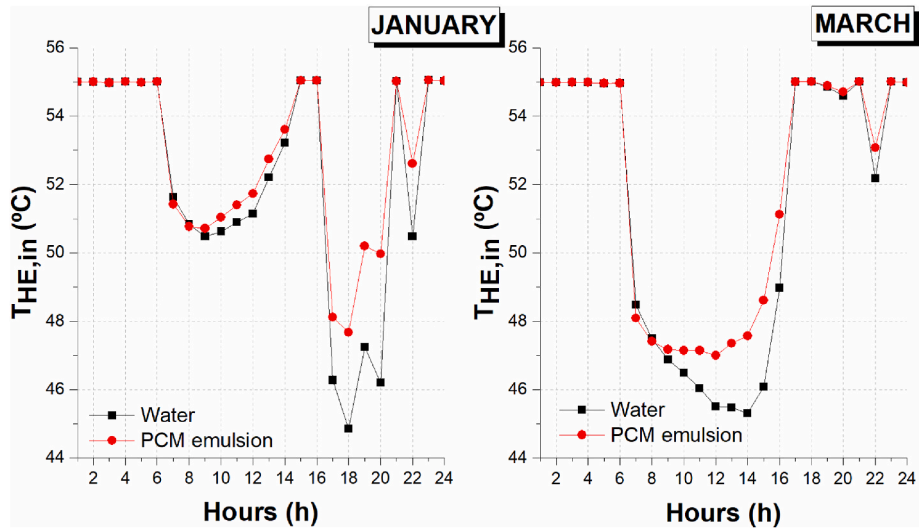

Fig. 8. Inlet temperature of the DH in the customers' PHE for January (left) and March (right).

3.2.1. Performance with the same settlement

When the simulation is executed with the PCM emulsion while keeping the volume of the TES unit, one important consequence is the reduction of the obtained value of $\dot{m}_{max,sto}$ [h] and so the reduction of the number of coils to 14, which entails an investment cost reduction. Trying different values of f_{st}, a value of the global coefficient transmission, U, similar to the case of TES with water has been achieved. The main parameters of each tank element, composed of a coil and a stirrer, are collected in Table 5.

Another relevant consequence is the stabilization of the storage temperature, that improves the performance of the whole system allowing to reduce the mass flow inside the coils, $\dot{m}_{sto}[h]$, during the discharge, as can be observed in Fig. 7, and to increase the temperature of the water sent to the customers PHE, as shown in Fig. 8. The consequences of levelling the temperatures are a more regular operation and an easier control of the mass flow variations, avoiding abrupt transients and enlarging the time life of the component of the whole facility.

In conclusion, the replacement of water with the PCM emulsion in the same configuration brings relevant enhancement in the overall operation of the considered system. Conserving the same nominal DH power than that one evaluated when studying water as storage material, with the same volume of material in the tank, is possible to store a

Table 6
Heat transfer study of the PCM emulsion in a tank with $V_{sto,eff}$ (130 m^3) of 20 internal coils.

Geometric variables		Heat transfer	
D_{st}(m)	0.75	Re_e	10087
D_{tank}(m)	1.23	Pr_{em}	3155
D_{coil}(m)	0.80	Nu_e	3139
N_{st}(rpm)	220	α_e(W/(m^2·K))	1022
ε	0.87	U(W/(m^2·K))	827.4

significant greater amount of thermal energy. Additionally, cost savings in the construction phase are generated by the diminished number of tank coils equipped.

3.2.2. Minimization of the TES volume

A different approach is to look for a minimum volume of the TES unit necessary to keep the same DH nominal power. This minimum value attainable is 130 m^3, because under this value the TES is not able to deliver the energy needed to the additional twenty buildings, and to guarantee the required $T_{HE,IN}$ threshold throughout the year. Table 6 collects the dimensions of the storage elements (one for each coil and stirrer), as well as the heat transfer values.

Table 7

$\dot{Q}_{av}$ [m] with $V_{sto,eff}$ = 180 m^3 reduction and corresponding reduction relative to $\dot{Q}_{peak}$ [m] using PCM emulsion and water.

	January	February	March	April	October	November	December
$\dot{Q}_{av,em}/$ kW	975.0	735.0	450.0	160.0	120.0	560.0	1115.0
$\dot{Q}_{av}/$ kW	1010.0	760.0	465.0	160.0	120.0	580.0	1190.0
$\dot{Q}_{peak}/$ kW	1462.9	1176.1	798.4	298.0	171.1	920.6	1823.0
% Red	33.35	37.50	43.64	46.31	29.87	39.17	38.83

Table 8

$\dot{m}_{DH,nom}$[m] with $V_{sto,eff}$ = 180 m^3 comparison between system using water or the PCM emulsion.

	January	February	March	April	October	November	December
$\dot{m}_{DH,em}/$ (kg /s)	11.66	8.792	5.383	1.914	1.435	6.669	13.94
$\dot{m}_{DH,w}/$ (kg /s)	12.081	9.091	5.562	1.914	1.435	6.938	14.234

Table 9

Heat transfer study of the PCM emulsion in a tank with $V_{sto,eff}$ (180 m^3) of 21 internal coils.

Geometric variables		Heat transfer	
D_{st}(m)	0.75	Re_e	9728
D_{tank}(m)	1.34	Pr_{em}	3272
D_{coil}(m)	0.80	Nu_e	3302
N_{st}(rpm)	220	α_e(W/(m^2·K))	989
ε	0.865	U(W/(m^2·K))	805

From the calculation of the system performance in January, it was obtained that the necessary number of coil elements was 20. With the reduction of the storage size, the tank elements considered in the heat transfer study have been re-dimensioned. A smaller diameter of the tank element permits to achieve a better flow field produced by the selected stirrer and, consequently, a higher heat transfer effectiveness between the coils and the PCM emulsion. This enhancement is visible in the incremented value of Re_{em} and the reduced value of Pr_{em}, caused by the lower effective viscosity obtained.

The hourly profile of the storage temperature is now very close to the water used as storage medium. The same trend is found in the mass flows and the water temperature supplied to the customers' PHE. Despite the volume reduction, higher energy is still accumulated in the TES with the PCM emulsion. However, the tank size cannot be decreased anymore for satisfying the minimum THE,in prerequisite. So, under this approach the advantage attained with the emulsion is moved to the structural and economical point of view, being very slight the overall system operation improvement.

3.2.3. Minimization of DH nominal power demanded

As the main purpose of this application is the reduction of the nominal DH power demanded, the third and main approach is to calculate the reduction in this demand with the same tank volume of PCM emulsion instead of water. Applying the restrictions posed in section 2.3.2, the new values of $\dot{Q}_{av}$[m] are calculated and compared with the values for the TES with water. Table 7 lists the results, showing a noticeable reduction in the nominal power required to the network for all months but April and October, when further reductions have not been possible, mainly due to the insufficient exploitation of the storage and to the low thermal demand. Note that Table 7 also shows the improvement achieved for the base case of water, in order to compare the two 180 m^3 TES solutions.

Table 8 shows the $\dot{m}_{DH,nom}$[m] accomplished either with water or the selected PCM emulsion as TES material and Table 9 lists the values of the geometrical and thermal parameters for the current option.

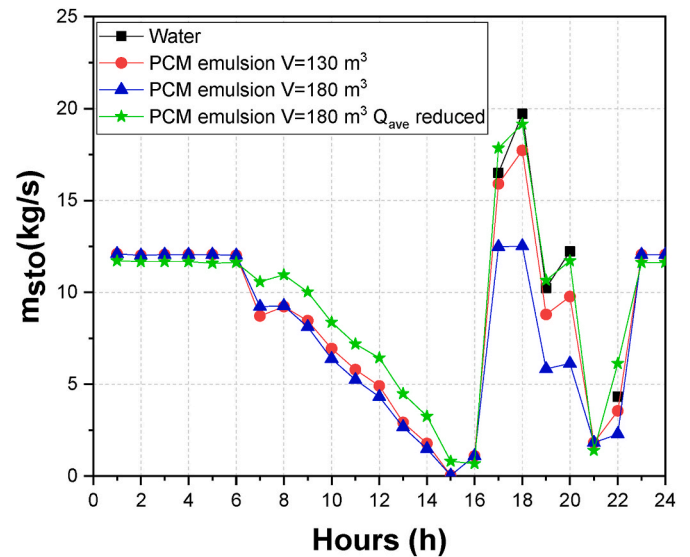As the power needs for space heating does not change, the reduction

Fig. 9. Storage mass flow comparison between the cases analysed (January).

of the nominal mass flow required to the DH network must be countervailed by a greater use of the TES unit, as Fig. 9 shows.

4. Conclusions

The integration of de-centralized TES into a DH system has been investigated in order to find out the possibility of the extension of the DH network to new buildings through new lines. A simple model has been formulated for the simulation of the integrated system. The outcomes obtained show that a de-centralized TES unit integrated into the DH grid is able to curtail the peak demand and, consequently, to reduce the mass flow that the network has to handle. This solution allows the connection of additional buildings in a saturated grid.

For what concern the additional "new" area, with a reasonable size of the connected tank it has been possible to maintain a regular nominal power supplied by the DH without raising the production during the peak hours. Furthermore, evaluating CHP-based DH system, this solution permits to move the heat production to the night where the electricity costs and requirements are lower. Additionally to the economic benefits, the installation of de-centralized storages allows the power unit to operate more regularly and provide the peak energy that otherwise should be supplied by auxiliary units (like boilers).

A more advanced and detailed study is needed in order to validate the model formulated. It has not been carried out any optimization

Table 10
Scenarios analysed and their general improvements.

Case	Medium TES	$V_{sto,eff}$	Coil elements	Improvements
1	Water	180 m^3	$N_{coil} = 22$ $D_{coil} = 0.6$ m	A reduction of 36.6 % in the nominal power to the DH network
2	PCM emulsion	180 m^3	$N_{coil} = 14$ $D_{coil} = 0.8$ m	Simpler tank (less coil elements) Smoother operation
3	PCM emulsion	130 m^3	$N_{coil} = 20$ $D_{coil} = 0.8$ m	Similar operation to the water tank Reduced tank size and cost
4	PCM emulsion	180 m^3	$N_{coil} = 21$ $D_{coil} = 0.8$ m	A reduction of 38.8 % in the nominal power to the DH network

because of the lack of economic and technical information. The design of the configuration utilized has been performed just respecting the hypothesis and prerequisites established according to the available data and the specific case treated. Several aspects have to be further analysed in order to confirm the feasibility of this solution. Firstly, the hydraulic transients, that the system has to perform, have to be characterized for ensuring their feasibility in the current configuration. A solution, that could help the hydraulic operation, could be the utilization of storage buffer units. However, also this strategy has to be developed in detail.

On the structural point of view, the construction of large volume storages equipped by several internal coils could be troublesome. A possible viable alternative is the utilization of several smaller units in parallel. Dealing with the PCM emulsion, this arrangement will probably facilitate the achievement of a homogeneous temperature field. The assumption of "fully-mixed" tank would be more real and the results achieved would better characterize the system operation.

By respect to the PCM emulsions as storage medium, the particular advantages are:

- Accumulate a greater amount of heat than water in the same configuration of the system, generating a smoother operation with less abrupt changes in the mass flow circulating in different hours.
- Reduce the storage volume and consequently the investment costs in order to achieve the same system operation than that attained using water.
- Reduce the nominal monthly DH power and, therefore, the additional mass flow that the existing DH pipes has to handle with the connection of the new area.

Table 10 shows the compilation of the four scenarios analysed together with their quantified improvements.

It is essential to acknowledge the potential of the PCM emulsion under research, especially because the emulsified paraffin is a by-product. Nevertheless, the enhancement of its thermophysical and rheological properties (including minimizing hysteresis, narrowing the phase change temperature range and improving phase change enthalpy) should be considered to optimize the TES performance. Indeed, this characteristic would generate a stronger temperature stabilization throughout the day, which allows a more regular overall operation of the DH network connected and smoother hydraulic transients.

CRediT authorship contribution statement

Giulia Rinaldi: Writing – original draft, Visualization, Software, Methodology, Investigation, Formal analysis, Data curation. **Ana Lazaro:** Supervision, Resources, Project administration, Funding acquisition, Conceptualization. **Monica Delgado:** Writing – review & editing, Validation, Methodology, Investigation, Data curation. **Jose Maria Marin:** Writing – review & editing, Validation, Software, Methodology. **Vittorio Verda:** Supervision, Conceptualization.

Declaration of competing interest

The authors declare that they have no known competing financial interests or personal relationships that could have appeared to influence the work reported in this paper.

Data availability

We can provide the EES code, but not the emulsion properties due to confidentiality issues

Appendix A. Supplementary data

Supplementary data to this article can be found online at https://doi.org/10.1016/j.energy.2024.132517.

References

[1] Olsthoorn D, Haghighat F, Mirzaei PA. Integration of storage and renewable energy into district heating systems: a review of modelling and optimization. Sol Energy 2016;136:49–64. https://doi.org/10.1016/j.solener.2016.06.054.

[2] Lund H, Möller B, Mathiesen BV, Dyrelund A. The role of district heating in future renewable energy systems. Energy 2010;35:1381–90. https://doi.org/10.1016/j.energy.2009.11.023.

[3] Köfinger M, Basciotti D, Schmidt RR, Meissner E, Doczekal C, Giovannini A. Low temperature district heating in Austria: energetic, ecologic and economic comparison of four case studies. Energy 2016;110:95–104. https://doi.org/10.1016/j.energy.2015.12.103.

[4] Lund H, Ostergaard PA, Chang M, Werner S, Svendsen S, Sorknaes P, Thorsen JE, Hvelplund F, Gram Mortensen BO, Mathiesen BV, Bojesen C, Duic N, Zhang X, Moller B. The status of 4th generation district heating: research and results. Energy 2018;164:147–59. https://doi.org/10.1016/j.energy.2018.08.206.

[5] Buffa S, Cozzini M, D'Antoni M, Baratieri M, Fedrizzi R. 5th generation district heating and cooling systems: a review of existing cases in Europe. Renew Sustain Energy Rev 2019;104:504–22. https://doi.org/10.1016/j.rser.2018.12.059.

[6] Guelpa E, Capone M, Sciacovelli A, Vasset N, Baviere R, Verda V. Reduction of supply temperature in existing district heating: a review of strategies and implementations. Energy 2023;262:125363. https://doi.org/10.1016/j.energy.2022.125363.

[7] Guelpa E, Verda V. Thermal energy storage in district heating and cooling systems: a review. Appl Energy 2019;252:113474. https://doi.org/10.1016/j.apenergy.2019.113474.

[8] Basciotti D, Schmidt RR. Peak reduction in distric heating networks- A comparison study and practical considerations. In: Proceedings from the 14th international Symposium on district Heating and cooling; 2014.

[9] Colella F, Sciacovelli A, Verda V. Numerical analysis of a medium scale latent energy storage unit for district heating systems. Energy 2012;45:397–406. https://doi.org/10.1016/j.energy.2012.03.043.

[10] Castro JF, Rossi A, Chiu JN, Martin V, Lacarriere B. Techno-economic assessment of active latent heat thermal energy storage systems with low-temperature district heating. International Journal of Sustainable Energy Planning and Management 2017;13:5–18. https://doi.org/10.5278/ijsepm.2017.13.2.

[11] Lee D, Jeong HJ, Ji HY, Park SY, Chung D-Y, Kang C, Kim KM, Park D. Peak load shifting control on hot wáter supplied from district heating using latent heat storage system in apartment complex. Case Stud Therm Eng 2022;34:101993. https://doi.org/10.1016/j.csite.2022.101993.

[12] Hlimi M, Lebrouhi BE, Belcaid A, Lamrani B, Balli L, Ndukwu MC, ElRhafiki T, Kousksu T. A numerical assessment of a latent heat storage system for district heating substations. J Energy Storage 2023;57:106210. https://doi.org/10.1016/j.est.2022.106210.

[13] Frederiksen S, Werner S. District heating and cooling. Studentlitteratur; 2013.

[14] Lauenburg P, Chapter 11. Temperature optimization in district heating systems, advanced district Heating and cooling (DHC) systems. Woodhead Publishing Series in Energy; 2016.

[15] Guidelines for Low-Temperature District Heating.Eudp 2010-II: full-scale demonstration of low-temperature district heating in existing buildings.

[16] Delgado M, Lázaro A, Mazo J, Peñalosa C, Dolado P, Zalba B. Experimental analysis of a low cost phase change material emulsion for its use as thermal storage system. Energy Convers Manag 2015;106:201–12. https://doi.org/10.1016/j.enconman.2015.09.033.

[17] Shao J, Darkwa J, Kokogianmakes G. Review of phase change emulsions (PCMEs) and their applications in HVAC systems. Energy Build 2015:200–17. https://doi.org/10.1016/j.enbuild.2015.03.003.

[18] Blumm J, Lindemann A, Min S. Thermal characterization of liquids and pastes using the flash technique. Thermochim Acta 2007;455:26–9. https://doi.org/10.1016/j.tca.2006.11.023.

[19] Dong S, Zhang M, Jin K, Yang R. An improved laser flash method for thermal conductivity measurement of molten salts. Prog Nat Sci: Mater Int 2024;34:345–53. https://doi.org/10.1016/j.pnsc.2024.03.006.

[20] Pietrak K, Wisniewski TS. A review of models for effective thermal conductivity of composite materials. Journal of Power Technologies 2015;95:14–24.

[21] Sakawa M. Chapter 13. Prediction and operational planning in district heating and cooling systems, *Advanced District Heating and Cooling (DHC) Systems*. Woodhead Publishing Series in Energy; 2016.

[22] Ortiga J, Bruno JC, Coronas A. Selection of typical days for the characterization of energy demand in cogeneration and trigeneration optimization models for

buildings. Energy Convers Manag 2011;52:1934–42. https://doi.org/10.1016/j.enconman.2010.11.022.

[23] Prabhanjan DG, Rennie TJ, Vijaya Raghavan GS. Natural convection heat transfer from helical coiled tubes. Int J Therm Sci 2004;43:359–65. https://doi.org/10.1016/j.ijthermalsci.2003.08.005.

[24] Fernandez-Seara, Diz R, Uhia FJ, Sieres J, Dopazo JA. Thermal analysis of a helically coiled tube in a domestic hot water storage tank. In: HEFAT 2007. 5th international Conference on heat transfer, fluid Mechanics and thermodynamics; 2007.

[25] Delgado M, Lazaro A, Mazo J, Penalosa C, Marin JM, Zalba B. Experimental analysis of a coiled stirred tank containing a low cost PCM emulsion as a thermal energy storage system. Energy 2017;138:590–601. https://doi.org/10.1016/j.energy.2017.07.044.

[26] Pollard J, Kantyka TA. Heat transfer to agitated non-Newtonian fluids. Transactions of the Institution of Chemical Engineers 1969;47:21–7.

[27] Metzner AB, Otto RE. Agitation of non-Newtonian fluids. AIChE J 1957;3:3–10. https://doi.org/10.1002/aic.69003010.